Tests of General Relativity with GWTC-3

LIGO-Virgo-KAGRA Webinar
27 January 2022

Testing GR paper
https://dcc.ligo.org/LIGO-P2100275/public
LVK, GWTC-3 testing GR paper
Data release
https://dcc.ligo.org/LIGO-P2100456/public

Speakers

Deirdre Shoemaker U Texas at Austin	Moderator
K. G. Arun Chennai Mathematical Institute	Introduction
Jenne Driggers LIGO Laboratory, Caltech	Data/Events
K. Haris Nikhef/Utrecht University	Consistency Tests
Marta Colleoni University of the Balearic Islands	Tests of generation, propagation and polarization
N. V. Krishnendu Albert Einstein Institute, Hannover/Leibniz University	Tests using the Remnant BH

Panelists

Peter Lott
Georgia Tech

Apratim Ganguly
IUCAA

Jan Steinhoff
AEI, Potsdam

Gregorio Carullo
U. Pisa

Abhirup Ghosh
AEI, Potsdam

Anna Puecher
Nikhef

Isaac Wong
CUHK


Introduction
Data/Events
Various
Tests of GR
Conclusions

Introduction

Gravitational Waves are unique probes of Strong-gravity

- Relativistic collisions of compact binaries provide a unique opportunity to test the validity of general relativity (GR) in a strong-field, radiative regime.
- Signatures of Beyond-GR physics would show up as modification to the dynamics of the binary, which can be tested using observations.
- We search for such deviations from GR using different methods, results of which are reported here.

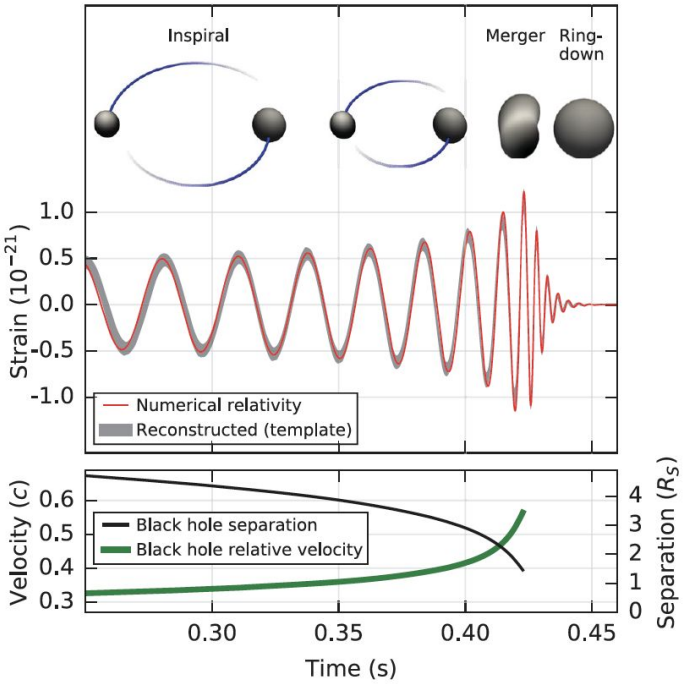

[B. P. Abbott et al. PRL 116, 061102, 2016]

Types of GR tests

We employ theory-agnostic tests, that do not rely on the predictions of any specific modified gravity theories, instead we test for possible deviations away from GR (null tests).

These tests may be broadly classified as

1. Consistency Tests
    a. Self-consistency of the signal
    b. Consistency of the signal with GR
2. Parameterized Tests
    a. Parameterize deviations from GR at the level of waveform and use the data to bound or constrain these additional parameters.

Through these tests, we probe the *generation, propagation and polarization* of GWs from various stages of a compact binary merger using the data from the second half of the third observing run (O3b).

Event selection and Parameter Estimation

Gravitational Wave observations to date

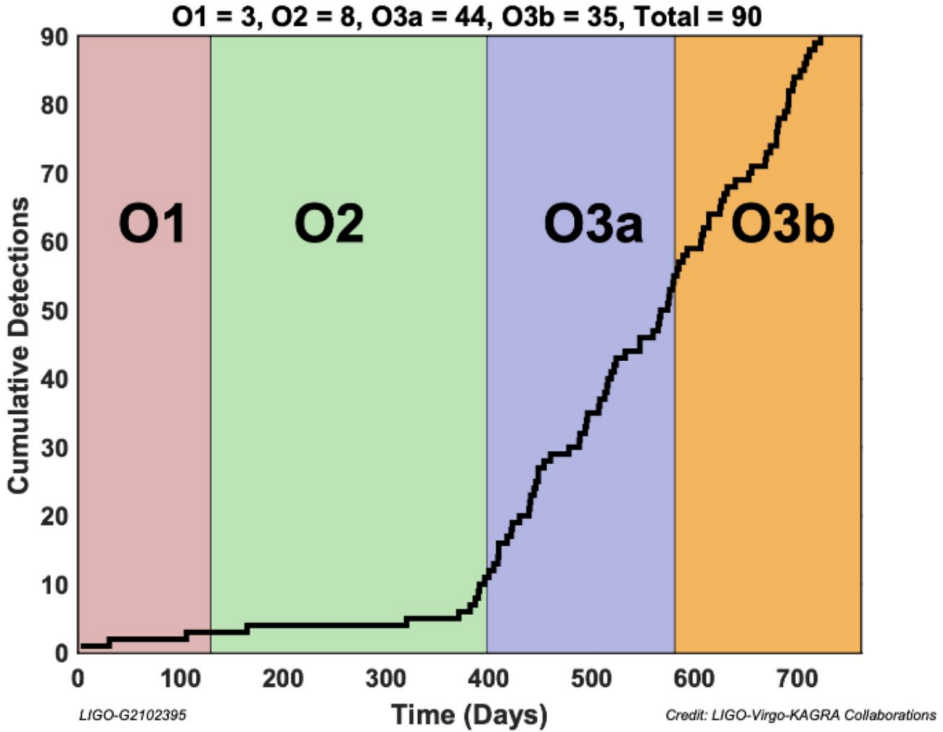

$P_{astro} > 0.5$

[LIGO-G2102395]

Event Selection

- 15 events with IFAR > 1000 yr are analysed from O3b.
- 14 BBHs + 1 NSBH (GW200115)
- Separate criteria for each analyses.
- Combine with events from GWTC-2, whenever possible.

TABLE II. List of O3b events considered in this paper. The first block of columns gives the names of the events and lists the instruments (LIGO **H**anford, LIGO **L**ivingston, **V**irgo) involved in each detection, as well as some relevant properties obtained assuming GR: luminosity distance $D_{\rm L}$, redshifted total mass $(1+z)M$, redshifted chirp mass $(1+z)\mathcal{M}$, redshifted final mass $(1+z)M_{\rm f}$, dimensionless final spin $\chi_{\rm f} = c|\vec{S}_{\rm f}|/(GM_{\rm f}^2)$, and network signal-to-noise ratio SNR. Reported quantities correspond to the median and 90% symmetric credible intervals, as computed in Table IV in GWTC-3 [81]. The final mass and final spin quantities are inferred from analysis of the entire signal and are for the remnant long after the coalescence and ringdown are complete, as described in [99]. The last block of columns indicates which analyses are performed on a given event according to the selection criteria in Sec. II: RT = residuals test (Sec. IV A); IMR = inspiral–merger–ringdown consistency test (Sec. IV B); PAR = parametrized tests of GW generation (Sec. V A); SIM = spin-induced moments (Sec. V B); MDR = modified GW dispersion relation (Sec. VI); POL = polarization content (Sec. VII); RD = ringdown (Sec. VIII A); ECH = echoes searches (Sec. VIII B).

Event	Inst.	Properties					SNR	Tests performed							
		$D_{\rm L}$ [Gpc]	$(1+z)M$ [$M_\odot$]	$(1+z)\mathcal{M}$ [$M_\odot$]	$(1+z)M_{\rm f}$ [$M_\odot$]	$\chi_{\rm f}$		RT	IMR	PAR	SIM	MDR	POL	RD	ECH
GW191109_010717	HL	$1.29^{+1.13}_{-0.65}$	140^{+21}_{-17}	$60.1^{+9.8}_{-9.3}$	135^{+19}_{-15}	$0.61^{+0.18}_{-0.19}$	$17.3^{+0.5}_{-0.5}$	✓	–	–	–	–	✓	✓	✓
GW191129_134029	HL	$0.79^{+0.26}_{-0.33}$	$20.10^{+2.94}_{-0.64}$	$8.49^{+0.06}_{-0.05}$	$19.19^{+3.07}_{-0.67}$	$0.69^{+0.03}_{-0.05}$	$13.1^{+0.2}_{-0.3}$	✓	–	✓	✓	✓	–	–	✓
GW191204_171526	HL	$0.65^{+0.19}_{-0.25}$	$22.74^{+1.94}_{-0.48}$	$9.70^{+0.05}_{-0.05}$	$21.60^{+2.05}_{-0.50}$	$0.73^{+0.03}_{-0.03}$	$17.5^{+0.2}_{-0.2}$	✓	–	✓	✓	✓	✓	–	✓
GW191215_223052	HLV	$1.93^{+0.89}_{-0.86}$	$58.4^{+4.8}_{-3.7}$	$24.9^{+1.5}_{-1.4}$	$55.8^{+4.8}_{-3.3}$	$0.68^{+0.07}_{-0.07}$	$11.2^{+0.3}_{-0.4}$	✓	–	–	–	✓	✓	–	✓
GW191216_213338	HV	$0.34^{+0.12}_{-0.13}$	$21.17^{+2.93}_{-0.66}$	$8.94^{+0.05}_{-0.05}$	$20.18^{+3.06}_{-0.70}$	$0.70^{+0.03}_{-0.04}$	$18.6^{+0.2}_{-0.2}$	✓	–	✓	✓	✓	✓	–	✓
GW191222_033537	HL	$3.0^{+1.7}_{-1.7}$	119^{+16}_{-13}	$51.0^{+7.2}_{-6.5}$	114^{+14}_{-12}	$0.67^{+0.08}_{-0.11}$	$12.5^{+0.2}_{-0.3}$	✓	–	–	–	✓	✓	✓	✓
GW200115_042309	HLV	$0.29^{+0.15}_{-0.10}$	$7.8^{+1.9}_{-1.8}$	$2.58^{+0.01}_{-0.01}$	$7.7^{+1.9}_{-1.8}$	$0.42^{+0.09}_{-0.05}$	$11.3^{+0.3}_{-0.5}$	✓	–	✓	–	–	–	–	✓
GW200129_065458	HLV	$0.90^{+0.29}_{-0.38}$	$74.6^{+4.5}_{-3.8}$	$32.1^{+1.8}_{-2.6}$	$70.9^{+4.2}_{-3.4}$	$0.73^{+0.06}_{-0.05}$	$26.8^{+0.2}_{-0.2}$	✓	✓	✓	✓	✓	✓	✓	✓
GW200202_154313	HLV	$0.41^{+0.15}_{-0.16}$	$19.01^{+1.99}_{-0.34}$	$8.15^{+0.05}_{-0.05}$	$18.12^{+2.09}_{-0.35}$	$0.69^{+0.03}_{-0.04}$	$10.8^{+0.2}_{-0.4}$	✓	–	✓	–	✓	–	–	✓
GW200208_130117	HLV	$2.23^{+1.00}_{-0.85}$	91^{+11}_{-10}	$38.8^{+5.2}_{-4.8}$	$87.5^{+10.3}_{-9.1}$	$0.66^{+0.09}_{-0.13}$	$10.8^{+0.3}_{-0.4}$	✓	✓	–	–	✓	✓	–	✓
GW200219_094415	HLV	$3.4^{+1.7}_{-1.5}$	103^{+14}_{-12}	$43.7^{+6.3}_{-6.2}$	98^{+13}_{-11}	$0.66^{+0.10}_{-0.13}$	$10.7^{+0.3}_{-0.5}$	✓	–	–	–	✓	✓	–	✓
GW200224_222234	HLV	$1.71^{+0.49}_{-0.64}$	$94.9^{+8.3}_{-7.2}$	$40.9^{+3.5}_{-3.8}$	$90.2^{+7.5}_{-6.4}$	$0.73^{+0.07}_{-0.07}$	$20.0^{+0.2}_{-0.2}$	✓	✓	–	–	✓	✓	✓	✓
GW200225_060421	HL	$1.15^{+0.51}_{-0.53}$	$41.2^{+3.0}_{-4.0}$	$17.65^{+0.98}_{-1.97}$	$39.4^{+2.9}_{-3.6}$	$0.66^{+0.07}_{-0.13}$	$12.5^{+0.3}_{-0.4}$	✓	✓	✓	✓	✓	✓	–	✓
GW200311_115853	HLV	$1.17^{+0.28}_{-0.40}$	$75.9^{+6.2}_{-5.7}$	$32.7^{+2.7}_{-2.8}$	$72.4^{+5.6}_{-5.1}$	$0.69^{+0.07}_{-0.08}$	$17.8^{+0.2}_{-0.2}$	✓	✓	✓	–	✓	✓	✓	✓
GW200316_215756	HLV	$1.12^{+0.47}_{-0.44}$	$25.5^{+8.7}_{-1.1}$	$10.68^{+0.12}_{-0.12}$	$24.3^{+9.0}_{-1.1}$	$0.70^{+0.04}_{-0.04}$	$10.3^{+0.4}_{-0.7}$	✓	–	✓	✓	–	–	–	✓

[R. Abbott et al. 2021]

Parameter Inference

- Different waveforms for different analyses, both with and without higher modes from the **Phenom** and **SEOB** families
  - SEOB : spinning effective-one-body, only aligned-spin models used in this work
  - Phenom: phenomenological waveforms, precessing (constructed via ‘twisting-up’ method)
- Standard LVK Parameter Estimation tools:
  - PE: LALInference, bilby, pyRing
  - BayesWave PSDs matching O3b catalogue GWTC-3
- Following O3aTGR, we present two types of combined bounds obtained assuming that:
  - Deviations take a common value for all sources (Restricted)
  - Deviations can vary across sources (Hierarchical)

Consistency Tests

Residuals Test

Are the residuals consistent with detector noise?

- Subtract off the best-fit (Max Likelihood) waveform from the data of each event and test whether the residuals are consistency with detector noise.
- Compute the coherent power in the residual data using BayesWave.
- Background analysis to compute *p-values*.
- Uses **IMRPhenomXPHM** model for the analysis.
- All the 15 events are analysed.

Results: Residual Analysis

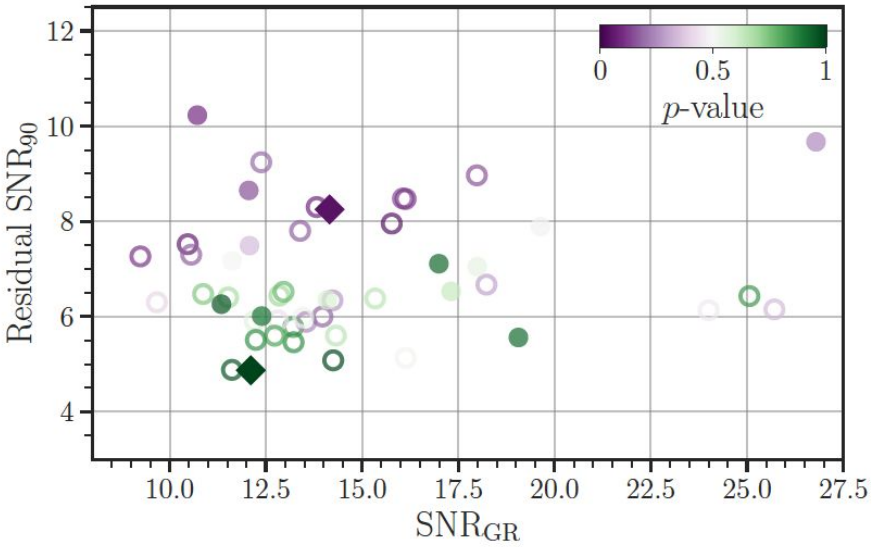

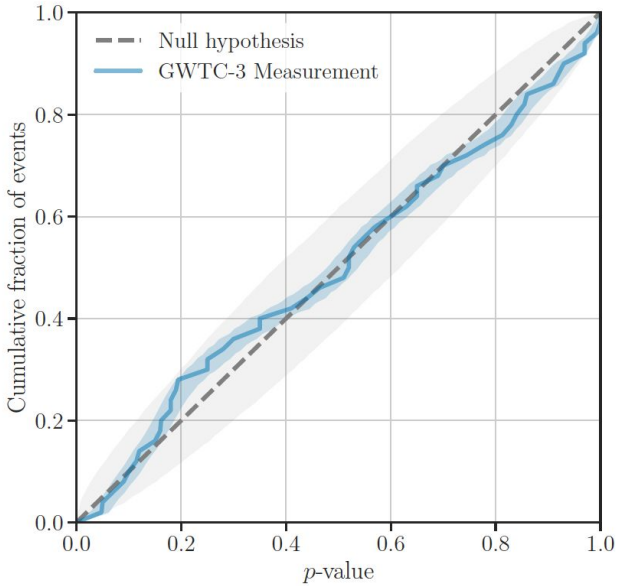

No evidence for violation of GR

[R. Abbott et al. 2021]

IMR Consistency test

Are the inspiral and post-inspiral parts consistent with each other?

The binary's final mass and spin parameters are measured separately from the low and high-frequency parts we then compare the two measurements to check their agreement.

Deviation Parameters

$$\frac{\Delta M_{\rm f}}{\bar{M}_{\rm f}} = 2\,\frac{M_{\rm f}^{\rm inspiral} - M_{\rm f}^{\rm postinspiral}}{M_{\rm f}^{\rm inspiral} + M_{\rm f}^{\rm postinspiral}}$$

$$\frac{\Delta \chi_{\rm f}}{\bar{\chi}_{\rm f}} = 2\,\frac{\chi_{\rm f}^{\rm inspiral} - \chi_{\rm f}^{\rm postinspiral}}{\chi_{\rm f}^{\rm inspiral} + \chi_{\rm f}^{\rm postinspiral}}$$

The parameter estimation is employed using IMRPhenomXPHM waveform model and the dynesty sampler available in Bilby.

[A. Ghosh et al. CQG 35 (1), 014002, 2017]

Results: IMR Consistency test

Event	f_c^{IMR} [Hz]	ρ_{IMR}	ρ_{insp}	ρ_{postinsp}	$Q_{\mathrm{GR}}^{\mathrm{2D}}$ [%]
GW200129_065458	136	25.7	20.1	16.0	1.5
GW200208_130117	98	9.9	7.2	6.8	10.5
GW200224_222234	107	19.4	14.3	13.1	20.7
GW200225_060421	213	12.9	11.1	6.6	1.3
GW200311_115853	122	17.5	13.5	11.0	15.2

Constraints on the final mass and spin parameters from individual events. Combined results are shown as grey histograms.

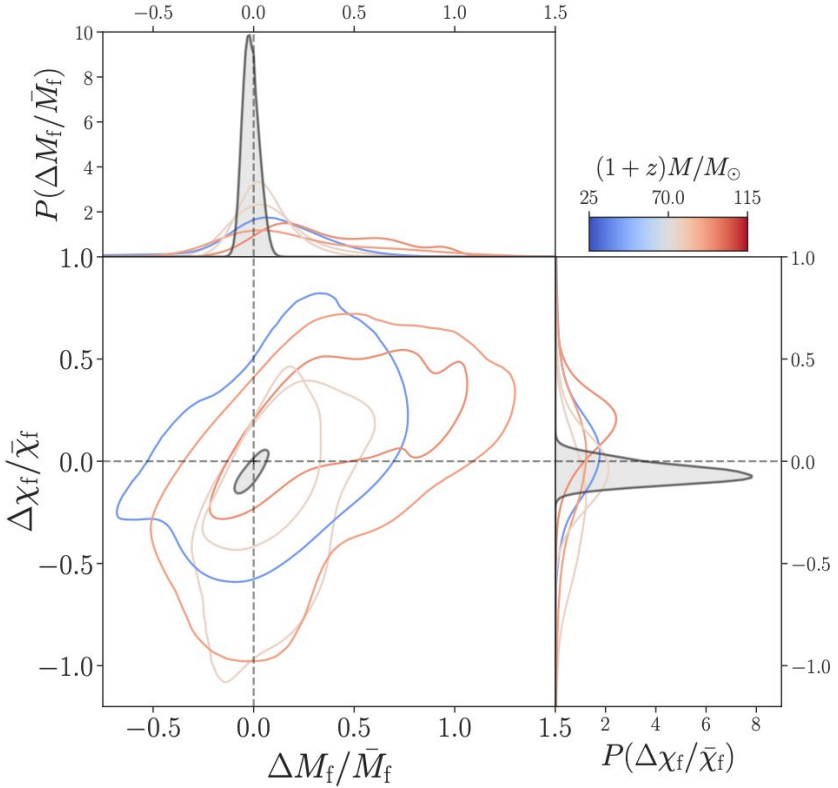

[R. Abbott et al. 2021]

Results: IMR Consistency test

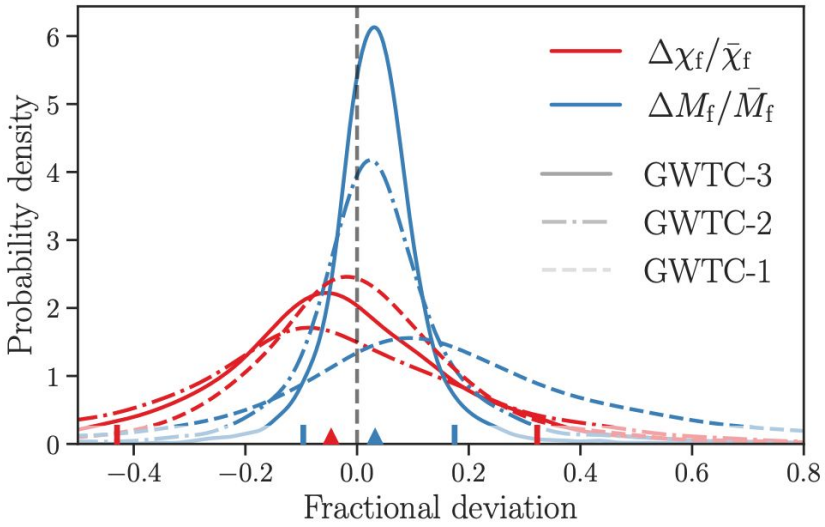

[R. Abbott et al. 2021]

Combined posteriors from hierarchical analysis. Results from previous catalogues are shown for comparison. The results are consistent with GR prediction.

Tests of GW generation

Tests of GW generation

- We perform two tests of GW generation:
  - Generic modifications : Additional fields and/or higher-order curvature corrections introduced in alternative theories of gravity will alter the binary's dynamics and hence the GW signal emitted.
  - Tests of spin-induced quadrupole moments: Different compact objects will have different spin-induced deformations based on their internal structure

Imprints on the GW phase

Tests of GW generation: Parameterized Tests of GR

Is the inspiral phase consistent with GR?

- Focus on the inspiral part of the waveform, which is well described by post-Newtonian (PN) theory
- In this framework, the GW phase can be written as a power series in terms of the frequency with each order being referred to as a PN order
- Introduce deviations at each PN order, one at a time, then compute their posterior distribution
- Besides the PN orders in GR, generic -1PN and 0.5PN deformation parameters are introduced. The former would be non-zero in the presence of dipole radiation
- Joint bounds are computed, combining O3b events with the events analysed in the previous observing runs.

Tests of GW generation: Parameterized Tests of GR

Is the inspiral phase consistent with GR?

- Introduce deviations in the phasing of SEOBNRv4_ROM, smoothly “turning them off” after a certain frequency cutoff
- Reparametrize the results as deviations in the phasing coefficients of a 3.5PN TaylorF2 phase:

$$\varphi_{\rm PN}(f) = 2\pi f t_{\rm c} - \varphi_{\rm c} - \frac{\pi}{4} + \frac{3}{128\eta}\left(\pi\tilde{f}\right)^{-5/3}\sum_{i=0}^{7}\left[\varphi_i + \varphi_{i\,l}\log(\pi\tilde{f})\right]\left(\pi\tilde{f}\right)^{i/3}$$

Terms scaling like $\approx \tilde{f}^{(-5+i)/3}$ at $i/2$-th PN order

Relative deviations if GR term is non-zero, absolute deviation otherwise

Lower (higher) order terms are predominant at low (high) frequencies

Tests of GW generation: Parameterized Tests of GR

Is the inspiral phase consistent with GR? YES!

- We combine the deviations from GR measured for each event and compute upper bounds on the deviation coefficients, by combining individual likelihoods
- Assume the deviation coefficients are the same across events
- -1PN bound improves roughly by a factor of 2!

NSBH candidate tightens constraint on $\delta\hat{\varphi}_{-2}$ (non zero in the presence of dipole radiation)

Consistency with GWTC-2 results

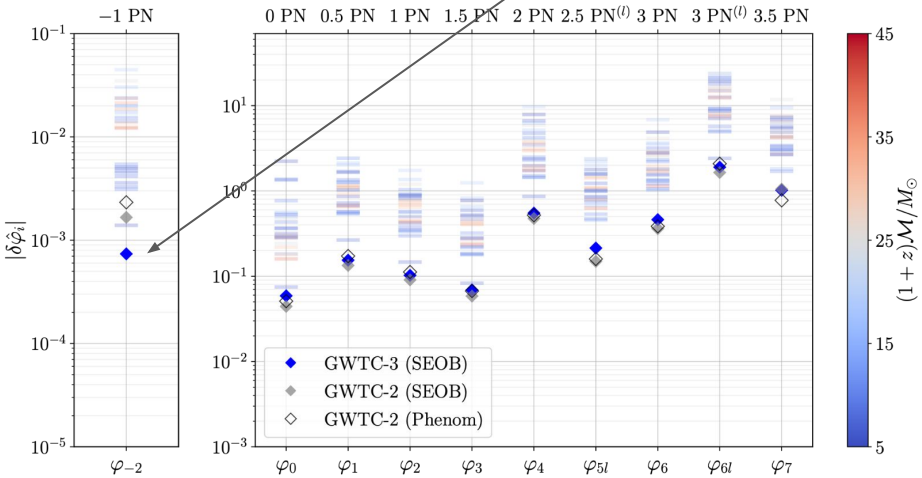

90% credible upper bounds

[R. Abbott et al. 2021]

Agathos+, PRD 89, 082001 (2014), LVK, PRD 103, 122002

Tests of GW generation: Parameterized Tests of GR

Is the inspiral phase consistent with GR? YES!

Hierarchical analysis results: assume the deviation coefficient can take different values for different events (filled distributions)

Joint-likelihood approach: deviation is the same for all events (unfilled distributions)

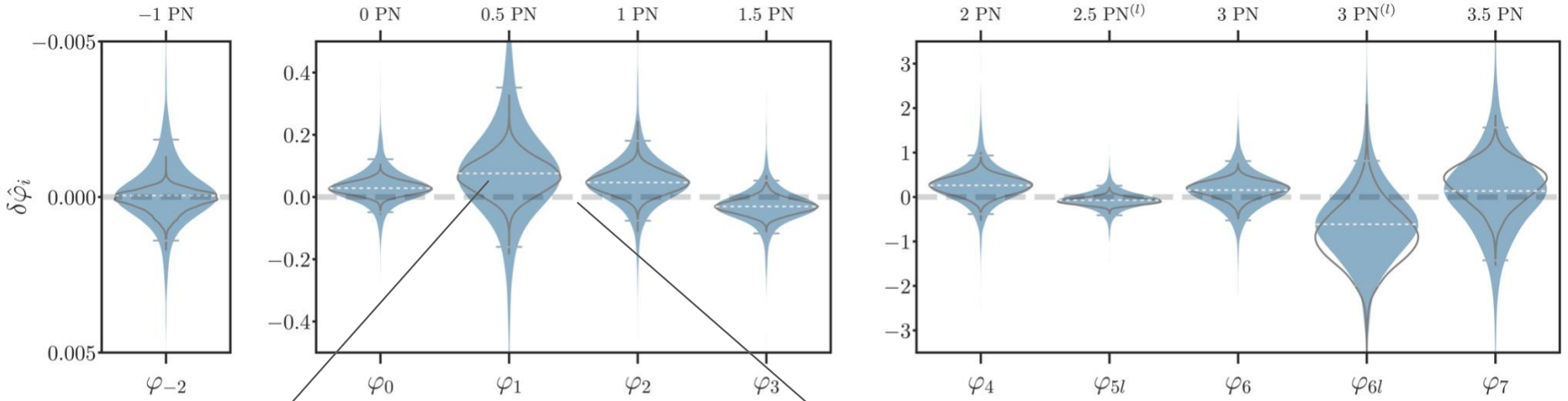

median

GR corresponds to $\delta\hat{\varphi}_i = 0$

[R. Abbott et al. 2021]

Tests of GW generation: Spin-induced quadrupole test

- Self spinning effects of compact objects lead to spin-induced deformations
- Direct imprints on the gravitational waveform as a leading order 2 post-Newtonian effect

$$Q = -\kappa \chi^2 m^3$$

The spin-induced quadrupole moment scalar is written in terms of the mass and spin parameters of the compact object

$\kappa = 1$ for Kerr black holes

$\kappa = \sim 2 - 14$ for neutron stars

$\kappa = \sim 10 - 150$ for boson stars

[William G. Laarakkers and Eric Poisson 1999 ApJ 512 282; Fintan D. Ryan; Phys. Rev. D 55, 6081,1997 Krishnendu et al. Phys. Rev. Lett. 119, 091101 (2017)]

Tests of GW generation: Spin-induced quadrupole test

Orbiting binary system characterized by its mass and spin parameters

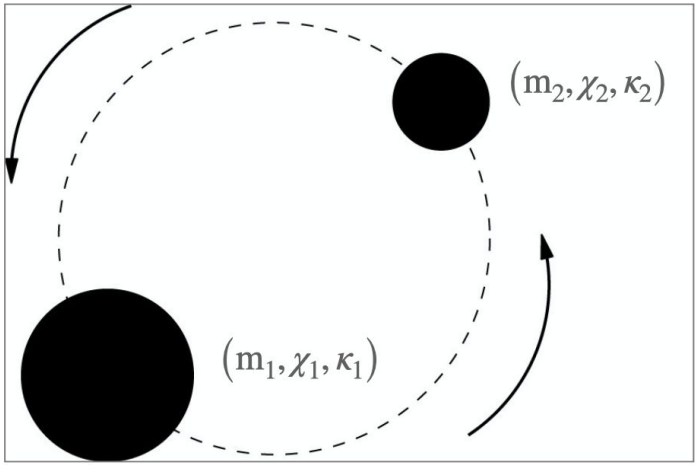

- We introduce parametric deviations of the form, $\kappa_1 = 1 + \delta\kappa_1$ and $\kappa_2 = 1 + \delta\kappa_2$.
- Measure the symmetric combination, $\delta\kappa_s$ assuming the antisymmetric combination vanishes, $\delta\kappa_a = 0$.
- By introducing these parameters into the waveform model as extra free coefficients to be constrained by the data.
- We analyse 6 new events passing our selection criteria using IMRPhenomPv2 waveform model and LALInference.

Results: Spin-induced quadrupole moment test

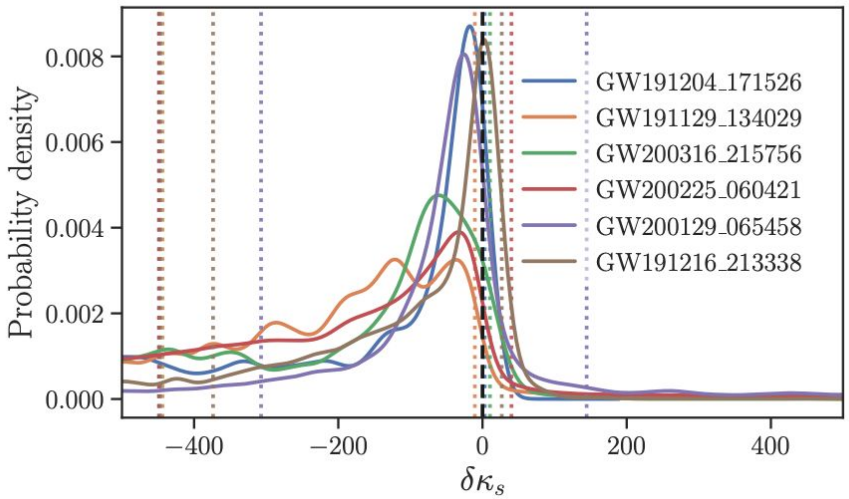

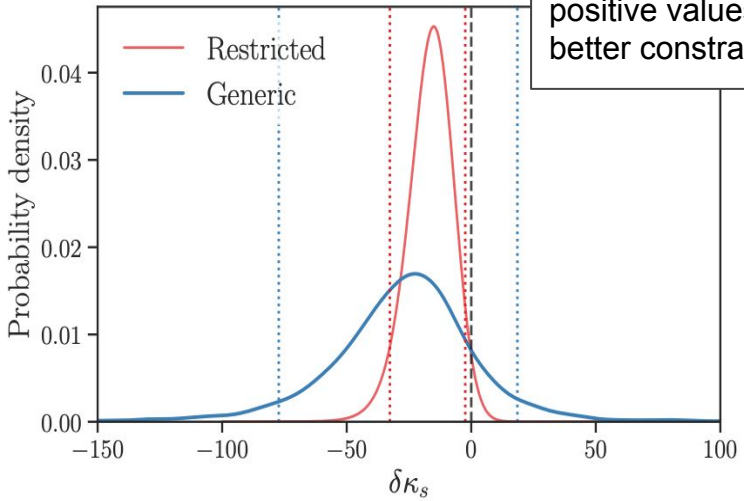

Correlation of $\delta\kappa_s$ with χ_{eff} means positive values are better constrained

[R. Abbott et al. 2021]

Constraints from individual events and by combining information from GWTC-2 and GWTC-3 events.

$$\log_{10} \mathcal{B}^{\text{Kerr}}_{\delta\kappa_s \neq 0} = 0.9 \quad (\delta\kappa_s \text{ symmetric})$$

$$\log_{10} \mathcal{B}^{\text{Kerr}}_{\delta\kappa_s \neq 0} = 2.2 \quad (\text{if } \delta\kappa_s > 0)$$

Tests of GW propagation

Tests for modified dispersion

- Gravitational waves in GR propagate non-dispersively at the speed of light.
- There are modified theories (massive graviton theories, Lorentz-violating theories), which predict dispersion of GWs.
- If there is dispersion, the different frequency components of the wave travel at different speeds and this affects the morphology of the signal
- This leads to an effective dephasing of the GW signal which can be measured
- Stronger effects for distant sources

Testing for modified Dispersion

Parameterized dispersion relation:

$$E^2 = p^2c^2 + A_\alpha p^\alpha c^\alpha$$

GR modification

- Bounds on A_α are obtained for different values of alpha, from 0 to 4 in steps of 0.5 (2 is excluded as it would be equivalent to a global time-shift of the signal)
- Bound on A_0 (for $A_0 > 0$) maps onto a bound on the mass of the graviton:

  $m_g = \sqrt{A_0}/c^2$
- We use IMRPhenomXP waveforms.
- We compute combined bounds from all events.

[Mirshekari et al. PRD 85, 024041, 2012, Clifford. M. Will PRD 57, 2061, 1998]

Results: Dispersion tests

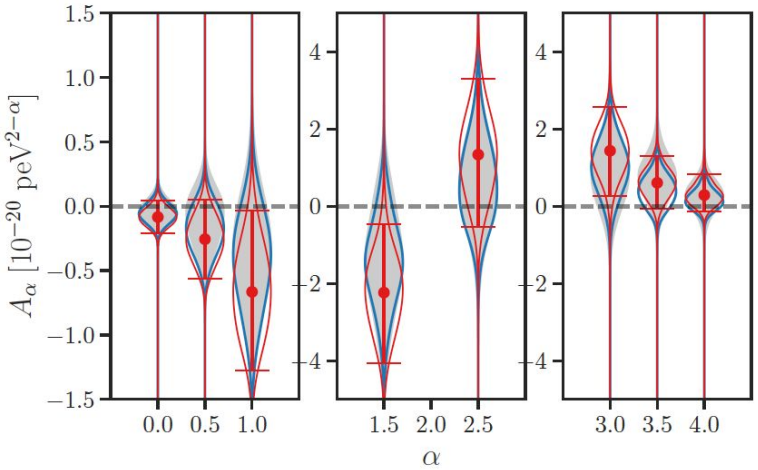

Gray: GWTC-2
Blue/Red: GWTC-3

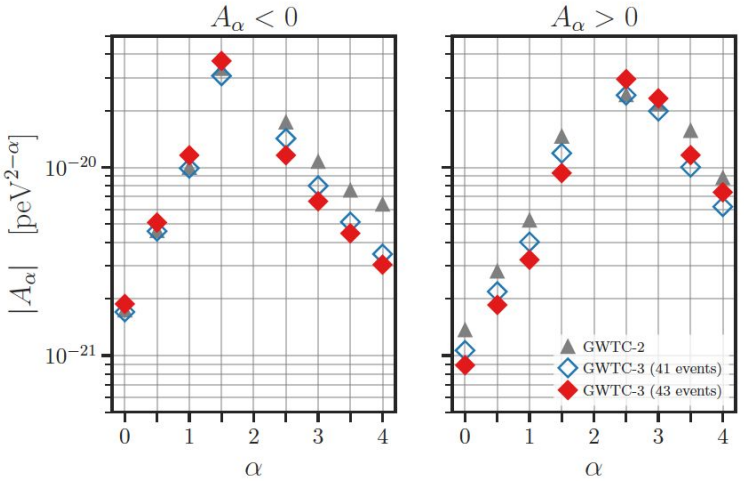

90% credible upper bounds

- On average: improvement over GWTC-2 in the upper bounds on deviation coefficients
- Improved bound on graviton mass with respect to GWTC-2 analysis

  $m_g < 1.27 \times 10^{-23}\ \mathrm{eV}/c^2$ (2.5 times better than Solar System bound)

[R. Abbott et al. 2021]

Tests of GW polarizations

GW polarizations

- A general metric theory of gravity admits up to 6 modes of GW polarizations: 3 transverse + 3 longitudinal.

- The network of GW detector allows us to probe non-GR polarization modes.

- **Null stream:** A linear combination of detector outputs which contains no GW signal (null projection).
- Waveform-agnostic
- Residual should be consistent with noise, if the assumed polarization hypothesis is correct

GR

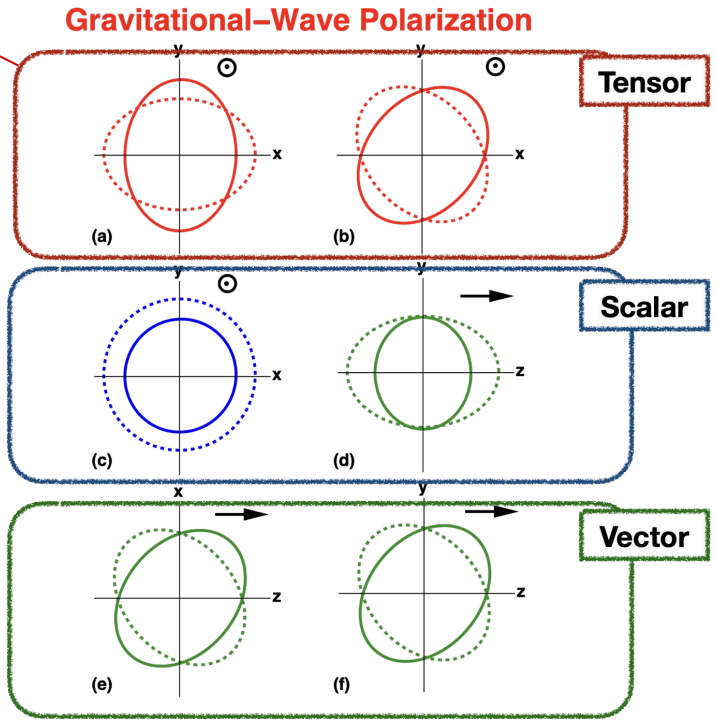

[Clifford M. Will, Living Rev. Relativity 17, 2014]

Results

- We test the presence of pure and mixed polarizations
- We perform the null projection with respect to a subspace spanned by 1 or 2 “basis modes” (does not need to coincide with the subspace of the hypothesis being tested)
- Combine all eligible events from O1+O2+O3 to get stronger bounds and compute Bayes factors to check if the data support non-GR polarizations

Events	$\log_{10}\mathcal{B}^{S}_{T}$	$\log_{10}\mathcal{B}^{V}_{T}$	$\log_{10}\mathcal{B}^{TS}_{T}$	$\log_{10}\mathcal{B}^{TV}_{T}$	$\log_{10}\mathcal{B}^{VS}_{T}$	$\log_{10}\mathcal{B}^{TVS}_{T}$
O1	-0.04 ± 0.07	0.09 ± 0.07	0.04 ± 0.07	0.09 ± 0.07	0.09 ± 0.07	0.07 ± 0.07
O2	-0.42 ± 0.12	0.04 ± 0.12	0.08 ± 0.12	0.22 ± 0.12	0.09 ± 0.12	0.35 ± 0.12
O3a	-1.85 ± 0.21	-1.04 ± 0.20	0.25 ± 0.20	0.07 ± 0.20	-1.05 ± 0.20	-0.18 ± 0.20
O3b	-1.93 ± 0.17	-0.79 ± 0.17	-0.17 ± 0.17	-0.07 ± 0.17	-0.86 ± 0.17	-0.32 ± 0.17
Combined	-4.24 ± 0.30	-1.70 ± 0.30	0.20 ± 0.30	0.31 ± 0.30	-1.73 ± 0.30	-0.08 ± 0.30

One basis-mode

Events	$\log_{10}\mathcal{B}^{V}_{T}$	$\log_{10}\mathcal{B}^{TS}_{T}$	$\log_{10}\mathcal{B}^{TV}_{T}$	$\log_{10}\mathcal{B}^{VS}_{T}$	$\log_{10}\mathcal{B}^{TVS}_{T}$
O1	–	–	–	–	–
O2	0.05 ± 0.03	0.01 ± 0.03	-0.02 ± 0.03	0.06 ± 0.03	0.01 ± 0.03
O3a	-0.37 ± 0.12	-0.77 ± 0.12	-0.72 ± 0.12	-0.73 ± 0.12	-0.91 ± 0.12
O3b	-0.09 ± 0.10	-0.22 ± 0.10	-0.35 ± 0.10	-0.38 ± 0.10	-0.38 ± 0.10
Combined	-0.41 ± 0.16	-0.98 ± 0.16	-1.09 ± 0.16	-1.05 ± 0.16	-1.29 ± 0.16

Two basis-modes

No evidence in favour of alternative polarization hypotheses

[Isaac C. F. Wong et. al. 2021, R. Abbott et al. 2021]

Remnant Properties and Ringdown tests

Black hole spectroscopy with the Remnant BH

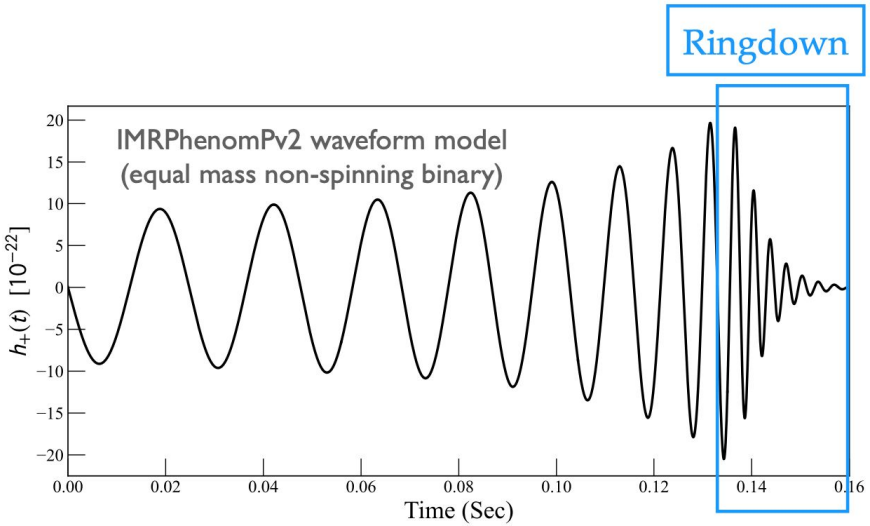

Schematic decomposition of post-merger signal

$$h_+(t) - ih_\times(t) = \sum_{\ell=2}^{+\infty} \sum_{m=-\ell}^{\ell} \sum_{n=0}^{+\infty} \mathcal{A}_{\ell mn} \exp\left[-\frac{t-t_0}{(1+z)\tau_{\ell mn}}\right] \exp\left[-\frac{2\pi i f_{\ell mn}(t-t_0)}{1+z}\right] {}_{-2}S_{\ell mn}(\theta, \phi, \chi_f),$$

[R. Abbott et al. 2021]

Black hole spectroscopy with the Remnant BH

Higher modes

Overtones

$$h_+(t) - ih_\times(t) = \sum_{\ell=2}^{+\infty} \sum_{m=-\ell}^{\ell} \sum_{n=0}^{+\infty} \mathcal{A}_{\ell mn} \exp\left[-\frac{t-t_0}{(1+z)\tau_{\ell mn}}\right] \exp\left[-\frac{2\pi i f_{\ell mn}(t-t_0)}{1+z}\right] {}_{-2}S_{\ell mn}(\theta, \phi, \chi_f),$$

Damping time of the mode

Oscillation frequency

- For astrophysical black holes in GR, the frequency and damping time are characterized by the mass and spin of the BH ***[final state conjecture]***
- BH spectroscopy: GW observations of BH mergers allow us to probe the properties of the remnant black hole and test the above conjecture.

[R. Penrose, Riv. Nuovo Cim. 1, 252 (1969), C. V. Vishveshwara Phys. Rev. D 1, 2870,R. Abbott et al. 2021, R. Abbott et al. 2020,Berti et al., 2009, Berti et al., 2005]

Ringdown analysis using pyRing

- **pyRing**: GW data analysis toolkit designed to perform parameter estimation and model selection of ringdown gravitational-wave signal in time domain.
- We perform the ringdown analysis using the three templates:
  - Kerr220: include $\ell = 2, |m| = 2, n = 0$
  - Kerr221: include $\ell = 2, |m| = 2, n = 0, 1$
  - KerrHM: include $m = \ell,\ m = \ell - 1$ modes with $\ell \leq 4$ and $n = 0$
- Parameter estimation using the three templates, parameterized ringdown analysis by modifying Kerr221 template and the Bayesian model selection

[pyring, Isi et al. PRL 123, 111102, 2019, Carullo et al. PRD 99, 123029, 2019]

Ringdown analysis using pyRing

$$\mathcal{O}_{\rm GR}^{\rm modGR} = \frac{1}{3}\left(\mathcal{B}_{\rm GR}^{\delta\hat{f}_{221}} + \mathcal{B}_{\rm GR}^{\delta\hat{\tau}_{221}} + \mathcal{B}_{\rm GR}^{\delta\hat{f}_{221},\delta\hat{\tau}_{221}}\right)$$

Event	Redshifted final mass $(1+z)M_{\rm f}$ $[M_\odot]$				Final spin $\chi_{\rm f}$				Higher modes	Overtones	
	IMR	$\rm Kerr_{220}$	$\rm Kerr_{221}$	$\rm Kerr_{HM}$	IMR	$\rm Kerr_{220}$	$\rm Kerr_{221}$	$\rm Kerr_{HM}$	$\log_{10}\mathcal{B}_{220}^{\rm HM}$	$\log_{10}\mathcal{B}_{220}^{221}$	$\log_{10}\mathcal{O}_{\rm GR}^{\rm modGR}$
GW191109_010717	$132.7^{+21.9}_{-13.8}$	$181.7^{+28.5}_{-30.6}$	$179.0^{+23.7}_{-21.7}$	$174.5^{+38.1}_{-30.1}$	$0.60^{+0.22}_{-0.19}$	$0.81^{+0.10}_{-0.24}$	$0.81^{+0.08}_{-0.14}$	$0.77^{+0.11}_{-0.21}$	−0.11	1.03	−0.27
GW191222_033537	$114.2^{+14.3}_{-11.7}$	$111.4^{+69.3}_{-29.7}$	$110.3^{+36.2}_{-23.8}$	$118.3^{+97.0}_{-46.2}$	$0.67^{+0.08}_{-0.10}$	$0.46^{+0.41}_{-0.41}$	$0.52^{+0.31}_{-0.43}$	$0.60^{+0.28}_{-0.66}$	0.08	−0.83	−0.20
GW200129_065458	$71.8^{+4.4}_{-3.9}$	$60.0^{+16.7}_{-8.9}$	$77.0^{+14.4}_{-14.2}$	$219.1^{+110.4}_{-140.0}$	$0.75^{+0.06}_{-0.06}$	$0.31^{+0.43}_{-0.28}$	$0.74^{+0.17}_{-0.59}$	$0.54^{+0.35}_{-0.59}$	−0.00	−0.47	−0.09
GW200224_222234	$90.3^{+6.4}_{-6.3}$	$84.4^{+23.2}_{-20.3}$	$88.6^{+15.5}_{-15.2}$	$119.4^{+142.6}_{-34.3}$	$0.73^{+0.06}_{-0.07}$	$0.61^{+0.27}_{-0.49}$	$0.60^{+0.23}_{-0.42}$	$0.64^{+0.27}_{-0.59}$	0.20	0.95	−0.11
GW200311_115853	$72.1^{+5.4}_{-4.7}$	$68.5^{+23.6}_{-13.5}$	$72.2^{+28.6}_{-16.3}$	$213.2^{+167.8}_{-141.5}$	$0.68^{+0.07}_{-0.08}$	$0.30^{+0.44}_{-0.28}$	$0.58^{+0.30}_{-0.47}$	$0.56^{+0.32}_{-0.54}$	0.02	−1.16	−0.15

- The remnant properties obtained from ringdown templates are consistent with their IMR counterparts.
- We find no evidence for higher modes. R. Abbott et al. 2021
- Among the events analysed, GW200224_222234 shows weak evidence for overtones.

Ringdown analysis using pyRing

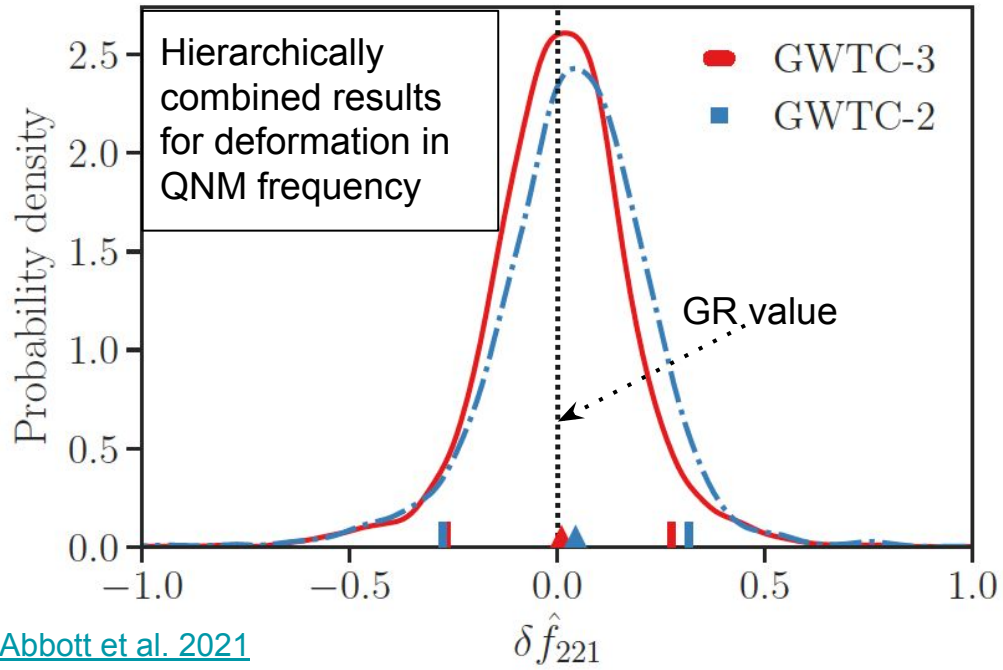

R. Abbott et al. 2021

- Parameter estimation analysis is performed on the modified Kerr221 template
- Parametric deviations to frequency and damping time parameters and are analysed along the GR parameters
- The deviation parameters are expected to be centered around zero

The frequency deviation parameter is found to be consistent with the GR prediction

Ringdown analysis using parameterized SEOB

- Ringdown analysis based on parameterized EOB model, SEOBNRv4HM (pSEOB)
- SEOBNRv4HM model predicts the frequency and damping time given the initial masses and spins

$$f^{\rm GR}_{\ell m 0} = f^{\rm GR}_{\ell m 0}(m_1, m_2, \chi_1, \chi_2)$$
$$\tau^{\rm GR}_{\ell m 0} = \tau^{\rm GR}_{\ell m 0}(m_1, m_2, \chi_1, \chi_2)$$

- In the pSEOB model, deviations in frequency and damping time are introduced as fractional deviations

$$f_{\ell m 0} = f^{\rm GR}_{\ell m 0}\,(1 + \delta \hat{f}_{\ell m 0})$$
$$\tau_{\ell m 0} = \tau^{\rm GR}_{\ell m 0}\,(1 + \delta \hat{\tau}_{\ell m 0})$$

- Along with the GR parameters, stochastic sampling is performed over $\{\delta \hat{f}_{220},\ \delta \hat{\tau}_{220}\}$ for events with SNR>=8 in the inspiral and post-inspiral regimes using LALInference.

[R. Abbott et al., 2021, Klein et al., 2018, R. Abbott et al 2020,Berti et al., 2009, Berti et al., 2005]

Ringdown analysis using parameterized SEOB

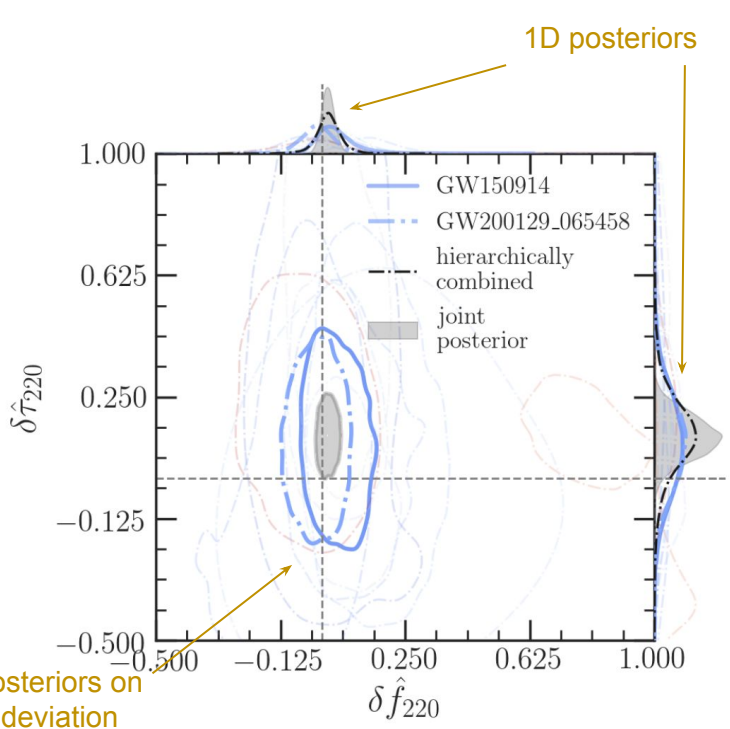

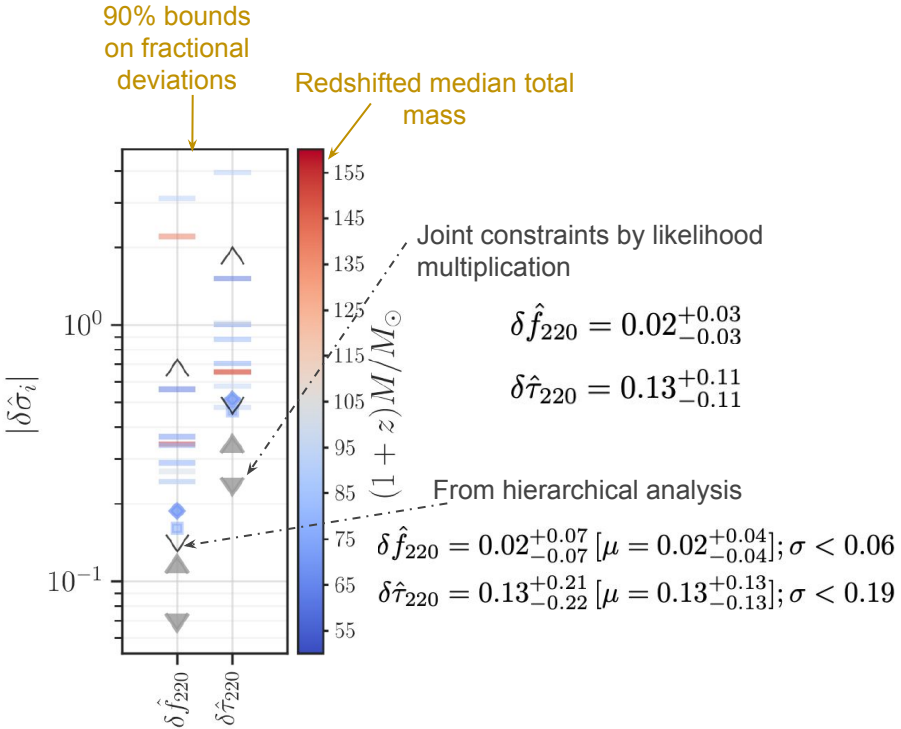

[R. Abbott et al., 2021, Klein et al., 2018, R. Abbott et al 2020,Berti et al., 2009, Berti et al., 2005]

Search for post-merger ‘Echoes’

- If the merger remnant is not a classical BH but an exotic compact object without an event horizon but a reflective surface, we expect GW emission as repeating pulses, known as echoes.

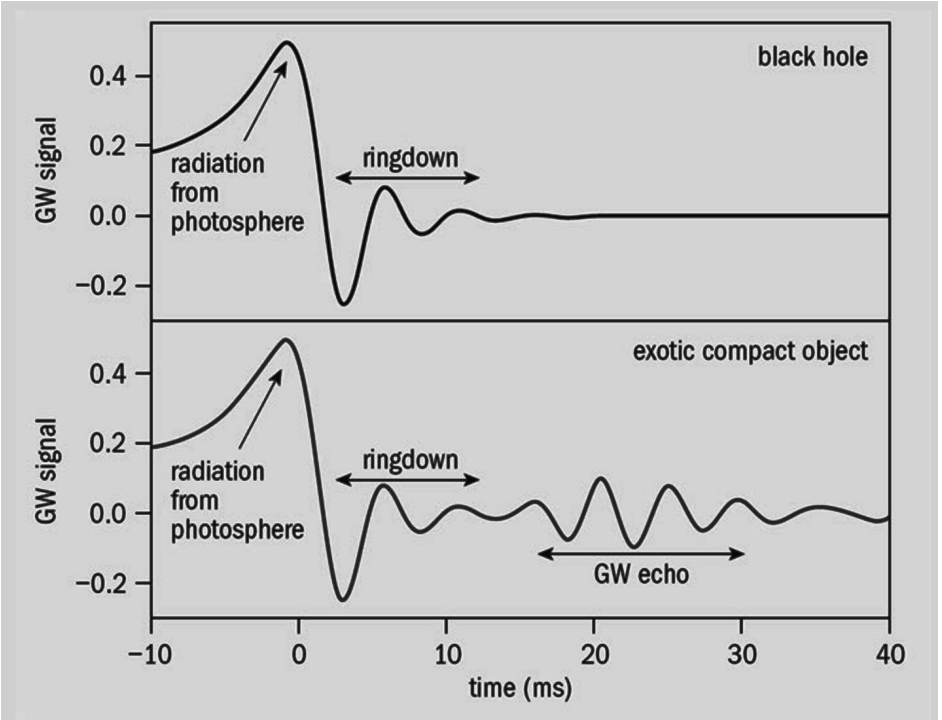

picture taken from cerncourier

Morphology independent test for GW echoes

- We search for post-merger echoes in a morphology independent way using the ***BayesWave*** algorithm employing a train of decaying sine Gaussians as wavelets.
- Signal Vs Noise Bayes Factors are computed for each event and we quantify the significance of them via *p-values* for each event.

P-P plot is consistent with the null hypothesis, indicating that we find no evidence for echoes.

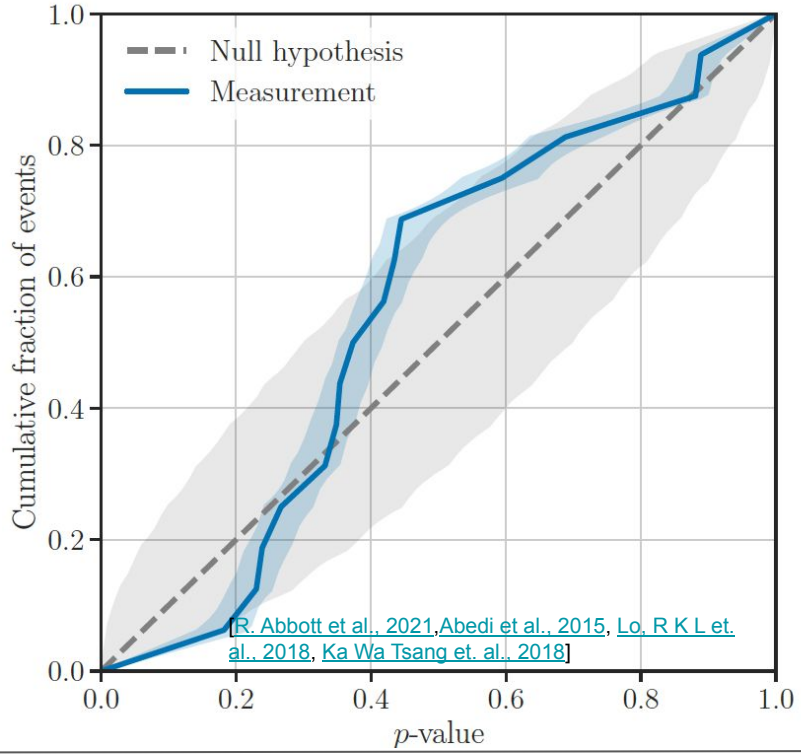

[R. Abbott et al., 2021,Abedi et al., 2015, Lo, R K L et. al., 2018, Ka Wa Tsang et. al., 2018]

Conclusions

- Tested for deviations from GR using nine different methods.
- Found no statistically significant evidence for any deviation from GR.
- Updated bounds on deformation parameters in the case of parameterized models/tests.
- Computed joint bounds wherever possible.

This material is based upon work supported by NSF's LIGO Laboratory which is a major facility fully funded by the National Science Foundation

PANEL